ELECTRONIC SUPPLEMENTARY INFORMATION

A Long-Wavelength Quantum Dot-Concentric FRET Configuration: Characterization and Application in a Multiplexed Hybridization Assay

Jia Jun Li and W. Russ Algar*

Department of Chemistry, University of British Columbia, 2036 Main Mall, Vancouver, British Columbia, V6T 1Z1, Canada

*Corresponding author: algar@chem.ubc.ca

Table of Contents

Additional Experimental Methods

Peptide labeling. Peptide (~0.25 mg, ~75 nmol) was dissolved in 5 μL of 50% v/v MeCN (*aq*) and mixed with either (i) 8 μL of thiol-reactive Alexa Fluor 680 C2 maleimide (11.1 mg mL^{-1}, ~90 nmol; Thermo-Fisher Scientific, Carlsbad, CA, USA) or (ii) 13 μL of thiol-reactive Alexa Fluor 633 C5 maleimide (11.1 mg mL^{-1}, ~111 nmol; Thermo-Fisher), both of which were dissolved in DMF. The reaction mixture was diluted to 100 μL with phosphate buffered saline (PBS; 10 mM, pH 7.0, 50 mM NaCl), vortexed, and agitated for 24 h at room temperature while protected from light. To purify the dye-labeled peptide from excess dye, the reaction mixture was loaded into a cartridge filled with Ni^{2+}-nitrilotriacetic acid (NTA)-agarose. The Ni^{2+}-NTA-agarose with bound peptide was washed with 2 × 10 mL PBS, 10 mL of PBS with 50% v/v EtOH, and another 2 × 10 mL PBS. The dye-labeled peptide was then eluted from Ni^{2+}-NTA using 3 × 0.5 mL portions of imidazole solution (300 mM in PBS; filtered through activated charcoal prior to use). The dye-labeled peptide in the imidazole eluate was then transferred to a cartridge filled with Amberchrom CG300M resin for desalting. After binding the dye-labeled peptide, the resin was washed with 4 × 10 mL of triethylammonium acetate (TEAA) buffer (0.2 M, pH 7.0) and subsequently eluted with 1 mL of 70% v/v MeCN (*aq*). The amount of dye labeled peptide was quantified by UV-visible spectrophotometry, split into 10 nmol fractions, and each fraction concentrated to dryness under vacuum.

Oligonucleotide labeling. These procedures applied to the block oligonucleotides (see Table 1). The oligonucleotides were received from the manufacturer (Integrated DNA Technologies; Coralville, IA, USA) with thiol linkers protected as disulfides.

A680 labeling. The disulfide of the as-received oligonucleotide (50 nmol) was reduced in 100 μL of tris(2-carboxyethyl)-phosphine (TCEP; 123 mM) in nuclease-free water for 1 h. The TCEP was removed by size-exclusion chromatography (SEC) with a NAP-10 column (GE Healthcare, Baie-d'Urfé, QC, Canada) using PBS (10 mM, pH 7.0, 50 mM NaCl) following the manufacturer's instructions. The oligonucleotide fraction of the column eluate was immediately added to 15 μL of Alexa Fluor 680 C2 maleimide (11.1 mg mL^{-1}, ~170 nmol) in DMF. The reaction mixture was vortexed and then agitated for 21 h at room temperature while protected

from light. Dye-labeled oligonucleotide was purified from excess dye through SEC with a Bio-Gel P-6 (Bio-Rad; Mississauga, ON, Canada) column using TEAA buffer (5 mM, pH 7.0). The purified A680-labeled oligonucleotide and its degree of labeling (~1:1) were quantified by UV-visible spectrophotometry, split into 10 nmol fractions, and each fraction concentrated to dryness under vacuum.

A633 labeling. Oligonucleotide (~50 nmol) was dissolved in 50 µL of water with 4% v/v triethylamine. Aqueous dithiothreitol (50 µL, 100 mM) was added and the mixture left at room temperature for 25 min. The solution was then extracted with six 400 µL portions of wet ethyl acetate. The aqueous phase was retained and diluted with 50 µL of PBS (100 mM, pH 7.4) before adding 15 µL of Alexa Fluor 633 C5 maleimide (11.1 mg mL^{-1}, ~130 nmol) in DMF. The reaction mixture was vortexed and then agitated for 20 h at room temperature while protected from light. The A633-labeled oligonucleotide was purified and quantitated as described above for labeling with A680.

Linker synthesis. A succinimidyl ester-activated dithiol linker (DTL; protected as a disulfide) was synthesized as summarized in Scheme S1, which is based on a published procedure[1] with minor modifications as described below.

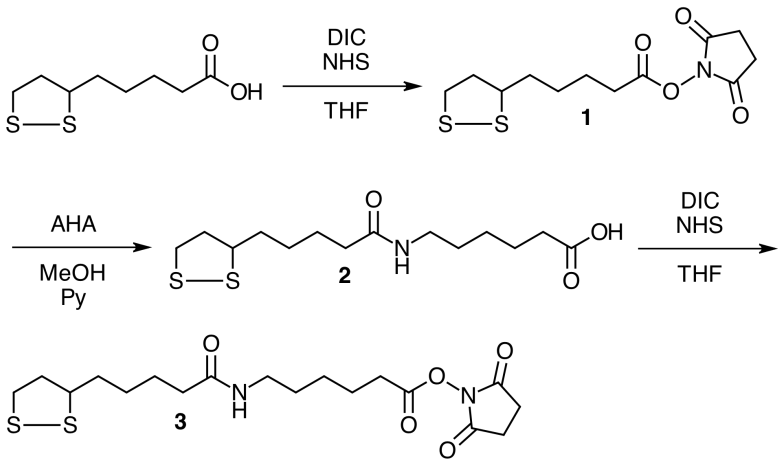

Scheme S1.

*Synthesis of **1***. Lipoic acid (2.0 g, 9.7 mmol) and *N*-hydroxysuccinimide (NHS; 1.38 g, 12 mmol) were dissolved in 60 mL of tetrahydrofuran (THF). *N*,*N′*-Diisopropylcarbodiimide (DIC; 1.9 mL, 12 mmol) was added to 5 mL of THF, and this solution was added dropwise to the solution of lipoic acid. The reaction was stirred for 5–6 h at room temperature and the resulting white precipitate was filtered by gravity. The filtrate was collected and concentrated to ~3 mL using a rotary evaporator before isopropanol was added and the mixture left at –20 °C overnight to crystallize **1**. The pale yellow crystals were collected by vacuum filtration, washed with ether, and dried. The product **1** (1.7 g , 5.6 mmol, 58% yield) was stored at –20 °C until needed.

*Synthesis of **2***. Compound **1** (0.60 g, 2.0 mmol) and 6-aminohexanoic acid (AHA; 0.50 g, 3.8 mmol) were added to a solution of 20 mL of anhydrous methanol (MeOH) mixed with 10 mL of pyridine (Py; dried over Na_2SO_4). The reaction mixture was then stirred overnight at room temperature. The product was extracted into dichloromethane (DCM; 50 mL) against an acidic aqueous phase (300–350 mL, 1–3 M HCl, 0.4–0.6 M NaCl). The organic phase was collected and washed three times with an acidic aqueous phase, then dried over sodium sulfate. The washed DCM layer was concentrated in a rotary evaporator until ~5 mL DCM remained, at which point 20 mL of diethyl ether was added. These concentration and dilution with ether steps were repeated three times to obtain solvent that was ~99% ether. The ether was then quickly evaporated to dryness under reduced pressure to obtain a pale yellow solid **2** (0.30 g, 0.94 mmol, 47% yield) that was stored at –20 °C until needed.

*Synthesis of **3***. Compound **2** (0.10 g, 0.31 mmol) was dissolved in THF with 1.2 equiv. of DIC and NHS. The synthesis of **3** was then done following the same procedure as the synthesis of compound **1**. The crystallized product **3** (0.080 g, 61% yield) was stored at –20 °C until needed.

Modification of oligonucleotides with linker. This procedure applies to the probe oligonucleotides (see Table 1), which were received from the manufacturer (Integrated DNA Technologies) with an amine-terminated alkyl linker. Compound **3** was dissolved in DMSO (40 µL of ~240 mM; ~9.6 µmol) and added to the oligonucleotide probe (100 µL of 500 µM; ~50 nmol) dissolved in borate buffer (25 mM, pH 8.5, ~50% DMSO). An additional 20 µL of DMSO was added to the reaction mixture, which was then left to mix for 24 h at room

temperature. Borate buffer (590 μL) was added to the reaction mixture to precipitate excess **3**. The mixture was centrifuged to pellet the precipitate and the supernatant was then loaded onto a NAP-10 column to remove any residual **3**. Oligonucleotide probe was quantified by UV-visible spectrophotometry, split into 20 nmol fractions, and each fraction was concentrated to dryness under vacuum.

Glutathione ligand exchange on QDs. QD605 (25 μL, ~200 μM) in toluene were diluted with 900 μL of chloroform. A solution of glutathione (GSH) dissolved in methanolic tetramethyl-ammonium hydroxide (TMAH; 300 μL, ~1 M GSH, 25% w/w TMAH) was then added. This mixture was vortexed and let stand at room temperature for 24 h. Borate buffer (200 μL; 50 mM, pH 9.5, 250 mM NaCl) was added. The mixture was vortexed then let phase separate to extract GSH-coated QDs into the aqueous phase. The organic layer was discarded, and the GSH-QDs were separated from excess GSH by precipitation: a volume of ~800 μL of ethanol was added, and the QDs were then centrifuged at ~5500 rcf for 4 min. The supernatant was discarded and the precipitated QDs were redispersed in 200 μL borate buffer (50 mM, pH 9.5, 250 mM NaCl). Three additional rounds of ethanol precipitation were repeated before final redispersion of the purified GSH-coated QDs in borate buffer (50mM, pH 8.5) at a concentration of ~30 μM.

Conjugation of QDs with oligonucleotide probe. QD605 (100 μL, 1 μM) were mixed with *P* equiv. of each linker-modified probe oligonucleotide (Prb 1, Prb 2) in tris-borate buffer (400 mM, pH 7.4, 50 mM NaCl) with TCEP (10 mM) for 20 h at room temperature. After this time, additional TCEP was added (2 μL, 100 mM) and the NaCl concentration was increased to 400 mM (with addition of a 5 M stock solution; referred to as salt aging). The mixture was left at room temperature for an additional 9 h. Unconjugated probe oligonucleotides were removed by purification on a Sephacryl S300 column with borate buffer (16 mM, pH 8.5) as the eluent. Typical reaction scales were between 100–300 μL. A 9 cm × 6 mm (length × diameter) column was sufficient for purification. Successful separation of unconjugated oligonucleotides was confirmed by UV-visible spectrophotometry. For the hybridization assays in Figure 7A, QD-probe oligonucleotide conjugates were prepared with $P = 15$ for both probes. For the displacement assays in Figure 7B, the QD-probe oligonucleotide conjugates were prepared with $P = 10$ for both probes.

Gel electrophoresis. Samples of conjugates were prepared as described in the main text. A 2 μL volume of 50% v/v (*aq*) glycerol was mixed with a 10 μL volume of conjugate sample before loading 12 μL into a well on a 1.0% w/v agarose gel. The gel was run at a field strength of 6.7 V cm^{-1} for *ca.* 25–30 min at room temperature in tris-borate buffer (100 mM, pH 8.3).

PL lifetime measurements. Time-resolved PL measurements were made with a streak camera system. Samples in a quartz cuvette were excited with laser pulses from an optical parametric generator (EKSPLA, Vilnius, Lithuania) pumped by a pulsed laser at 355 nm with a 10 Hz repetition rate and 35 ps pulse duration (EKSPLA). Time-resolved spectra were recorded with a combination of a spectrograph (Princeton Instruments, Trenton, NJ, USA) and streak camera (C7700; Hamamatsu Photonics, Hamamatsu, SZK, Japan) in photon counting mode. The excitation wavelengths were 464 nm for QD605, 570 nm for A633, and 610 nm for A680.

Hybridization and displacement assays. For hybridization assays, QD-probe oligonucleotide conjugates (40 μL, 50 nM) were incubated with the desired number of equivalents of dye-labeled block sequences in tris-borate buffer (200 mM, pH 7.4, 200 mM NaCl) for 1 h. PL emission spectra were measured by loading 35 μL of sample into the wells of a 384-well plate. The excitation wavelength was 464 nm and emission was measured between 500–850 nm (step size 2 nm).

For displacement assays, QD-probe oligonucleotide conjugates (100 nM) were mixed and hybridized with 10 equiv. of Blk 1(A633) and Blk 2(A680) in tris-borate buffer (200 mM, pH 7.4, 200 mM NaCl) for 1.5–2 h. Next, 20 μL aliquots of the block-hybridized conjugates were added to 20 μL volumes of solutions with different numbers of equivalents of Tgt 1 and Tgt 2. After mixing, the samples were left at room temperature for 1 h (the final concentration of QD conjugates was 50 nM). PL emission spectra were measured as noted for the hybridization assays.

Data analysis and crosstalk corrections. There was some crosstalk between the QD605 PL and the A633 PL, and between the A633 and A680 PL. This crosstalk was corrected prior to the calculation of PL ratios.

We define the peak PL emission intensity of a QD or dye, X, to be ${}_{X}I$. The raw PL intensity measured at a wavelength λ is defined as $I_{\lambda(\mathrm{nm})}$. For QD605-$(A633)_M$ samples, the crosstalk corrected PL intensities for the QD605 and A633 were calculated according to Eqns. S1–S2, where ${}_{X}\sigma_{\lambda}$ is a correction factor. The value of ${}_{X}\sigma_{\lambda}$ was determined from the PL emission spectrum of X, and represents the PL intensity at wavelength λ relative to the peak PL intensity of X at its emission maximum ($0 < {}_{X}\sigma_{\lambda} < 1$). The correction factors were ${}_{QD}\sigma_{648} = 0.018$, ${}_{A633}\sigma_{604} = 0.008$, ${}_{A680}\sigma_{648} = 0.011$, and ${}_{A633}\sigma_{704} = 0.272$. In some cases, consideration of only ${}_{QD}\sigma_{648}$ and ${}_{A633}\sigma_{704}$ was sufficient.

$$ {}_{\mathrm{QD}}I = I_{604} - {}_{A633}\,\sigma_{604}\left({}_{\mathrm{A633}}I\right) \tag{S1} $$

$$ {}_{\mathrm{A633}}I = I_{648} - {}_{\mathrm{QD}}\,\sigma_{648}\left({}_{\mathrm{QD}}I\right) \tag{S2} $$

Eqns. S1–S2 are a system of two equations and two unknowns that can be solved, which results in Eqn. S3. Calculation of Eqn. S3 permits direct calculation of Eqn. S1.

$$ {}_{\mathrm{A633}}I = \frac{I_{648} - {}_{\mathrm{QD}}\,\sigma_{648}\left(I_{604}\right)}{1 - {}_{\mathrm{QD}}\,\sigma_{648}\left({}_{\mathrm{A633}}\sigma_{604}\right)} \tag{S3} $$

For QD605-$(A680)_N$ samples, the PL emission peaks were sufficiently resolved that no crosstalk correction was necessary, as formalized by Eqns. S4–S5.

$$ {}_{\mathrm{QD}}I = I_{604} \tag{S4} $$

$$ {}_{\mathrm{A680}}I = I_{704} \tag{S5} $$

For QD605-$(A633)_M$-$(A680)_N$ samples, crosstalk between QD605 and A633, and between A633 and A680, was corrected using Eqns. S1, S6 and S7, which are a system of three equations and three unknowns:

$$ {}_{\mathrm{A633}}I = I_{648} - {}_{\mathrm{QD}}\,\sigma_{648}\left({}_{\mathrm{QD}}I\right) - {}_{\mathrm{A680}}\,\sigma_{648}\left({}_{\mathrm{A680}}I\right) \tag{S6} $$

$$ {}_{\mathrm{A680}}I = I_{704} - {}_{\mathrm{A633}}\,\sigma_{704}\left({}_{\mathrm{A633}}I\right) \tag{S7} $$

Eqns. S1, S6, and S7 can be solved to yield Eqn. S8. Calculation of Eqn. S8 permits direct calculation of Eqns. S1 and S7.

$$ {}_{A633}I = \frac{I_{648} - {}_{QD}\sigma_{648}\left(I_{604}\right) - {}_{A680}\sigma_{648}\left(I_{704}\right)}{1 - {}_{QD}\sigma_{648}\left({}_{A633}\sigma_{604}\right) - {}_{A680}\sigma_{A648}\left({}_{A633}\sigma_{704}\right)} \quad \text{(S8)} $$

Peak PL intensity ratios, $\rho_{dye/QD}$, were calculated according to Eqns. S9 and S10:

$$ \rho_{A633/QD} = {}_{A633}I \big/ {}_{QD}I \quad \text{(S9)} $$

$$ \rho_{A680/QD} = {}_{A680}I \big/ {}_{QD}I \quad \text{(S10)} $$

Average signal-to-background ratios. To compare the utilities of the QD605-A633-A680 and QD520/QD525a-A555-A647 cFRET configurations in serum and blood matrices, the average signal-to-background (S/B) ratios were calculated for the four samples: (0, 0), (12, 0), (0, 12), and (12, 12). The signal-to-background ratio was calculated for each sample at each wavelength in three steps. First, the measured PL spectrum for the serum or blood matrix was subtracted from the measured PL spectrum for a (*M*, *N*) configuration. This background-corrected spectrum was the divided by the PL spectrum for the matrix at each wavelength. Finally, the resulting S/B ratios for the four samples were averaged at each wavelength. These averaged values are plotted in Figure 6C.

Additional Results and Discussion

PL lifetimes. PL lifetimes for the QD605, A633, and A680 are listed in Table 2. PL intensity decay curves are shown in Figure S1. The QD605 PL decay was fit with a biexponential lifetime (2.6 ns, 16%; 14.6 ns, 84%) and the amplitude weighted average lifetime is given in Table 1. The dye PL decays were adequately fit with monoexponential lifetimes.

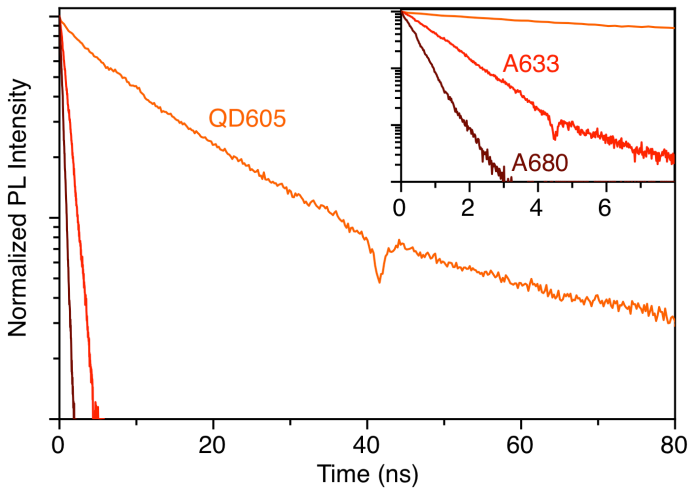

Figure S1. PL decay curves for directly excited QD605, Pep(A633), and Pep(A680). The dip in the data near 40 ns (and 4 ns in the inset) is a detector artifact. The inset is an expanded view of the data between 0–8 ns.

Quantum yield data. Unknown quantum yields (Φ_X) were determined relative to reference standards (Φ_{std}) by plotting measured fluorescence (F) versus measured absorbance (A) at the excitation wavelength. Eqn. S11 shows how the slopes of these plots relate to the quantum yields, where η is the refractive index of the solvent. The sulfo-Cy5 quantum yield was measured in ethanol. All other quantum yields were measured in aqueous buffer.

$$\Phi_X = \Phi_{std} \frac{F_X}{A_X} \frac{A_{std}}{F_{std}} \frac{\eta_X^2}{\eta_{std}^2} \tag{S11}$$

For the QD605, the reference standard was fluorescein in 0.10 M NaOH (*aq*) ($\Phi = 0.79$)[2] and both emitters were excited at 464 nm. For the A680 and A633, the quantum yield was measured with sulfo-Cy5 as the reference standard ($\Phi = 0.20$ as per the manufacturer; Lumiprobe Inc., Hallandale Beach, FL, USA)[3] and excitation at 600 nm. The measured quantum yields are tabulated in Table 1. The raw data is shown in Figure S2. The measured value for Blk 2(A680) ($\Phi = 0.31$) was close to the value reported by the manufacturer ($\Phi = 0.36$; Thermo-Fisher). The manufacturer does not report a value for A633.

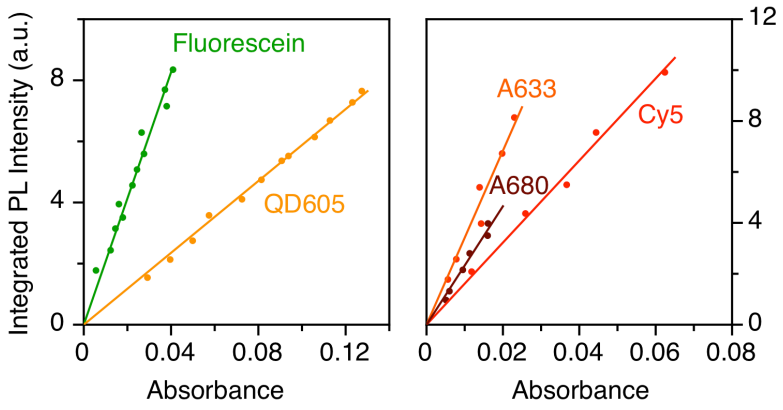

Figure S2. Plots of integrated PL intensity versus absorbance for (left) QD605 with a fluorescein reference, and (right) A633 and A680 with a sulfo-Cy5 reference.

Gel electrophoresis of peptide conjugates. Figure S3 shows a PL image of an agarose gel that confirms self-assembly of the polyhistidine terminated peptides, Pep(A633) and Pep(A680), to the shell of the QD605. The electrophoretic mobility of the QDs decreased as more peptides were assembled.

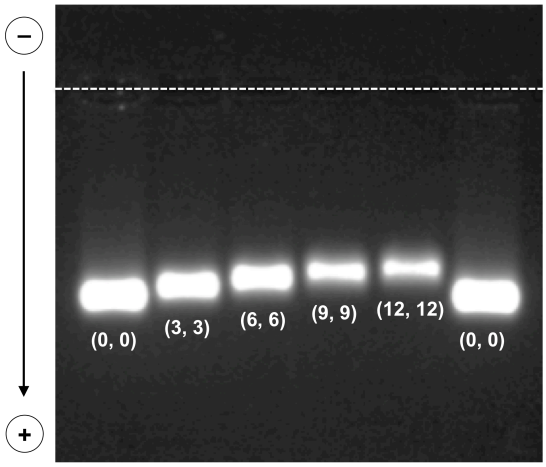

Figure S3. PL image of an agarose gel showing changes in the electrophoretic mobility of QD605-$[Pep(A633)]_M$-$[Pep(A680)]_N$ conjugates as the values of *M* and *N* increase. The average number of each peptide per QD is indicated by (*M*, *N*). The dashed line marks the position of the sample wells. The polarity of the applied electric field is indicated at the left along with the direction of migration.

PL emission spectra. Figure S4 shows a representative set of 25 PL emission spectra for QD605-[Pep(A633)]$_M$-[Pep(A680)]$_N$ cFRET samples, as well as control samples for the corresponding M × Pep(A633) and N × Pep(A680) samples.

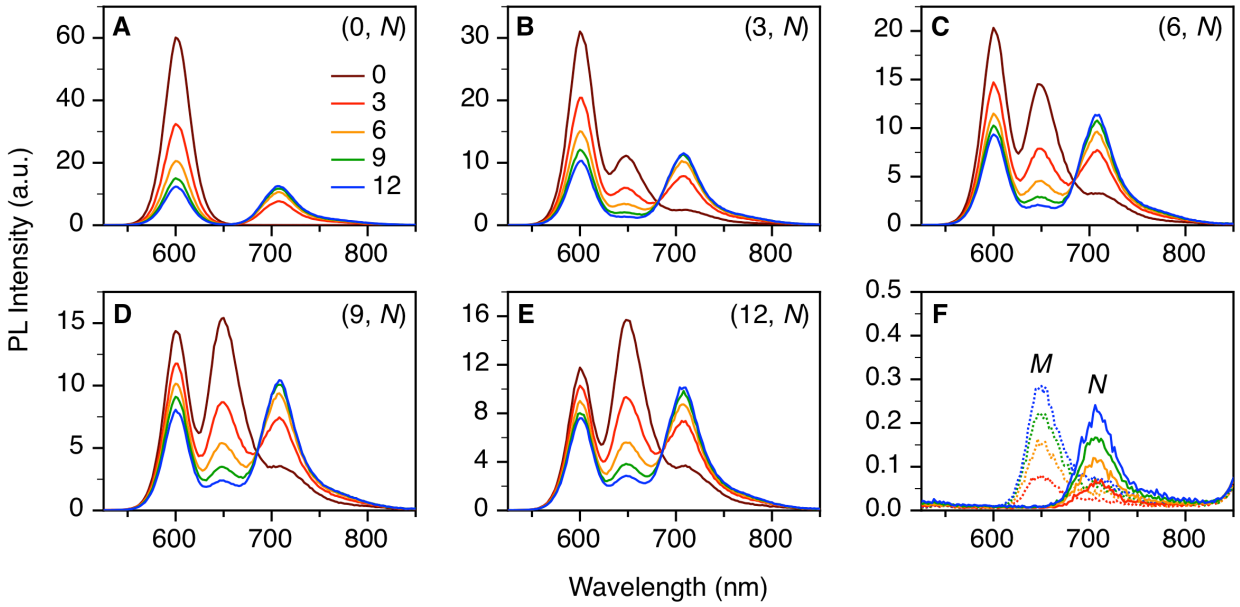

Figure S4. PL emission spectra (464 nm excitation) for **(A)-(E)** the QD605-[Pep(A633)]$_M$-[Pep(A680)]$_N$ cFRET configurations, and **(F)** the corresponding M × Pep(A633) and N × Pep(A680) samples. The configurations are denoted by the shorthand (M, N) notation. The legend in panel A applies to all other panels. Note the difference in the PL intensity scale for panel F.

Photobleaching of QD520-A555-A647. Figure S5 shows changes in PL from (0, 0), (12, 0), (0, 12), and (12, 12) samples of QD520-[Pep(A555)]$_M$-[Pep(A647)]$_N$ under continuous illumination at 400 nm. The QD520 in the (0, 0) sample exhibited ~20% photobrightening before slow photobleaching reduced its PL intensity to ~90% of its initial value after 50 min. The illumination power was ~50 mW at the sample. The illumination power was lowered to ~10 mW at the sample for subsequent measurements. For the (12, 0) sample, the QD520 and A555 PL tracked with one another and were both resistant to photobleaching. In contrast, for the (0, 12) sample, the A647 photobleached at a rate of 0.08 min^{-1}, and the QD520 PL intensity increased by ~100% in parallel with bleaching of the A647. For the (12, 12) sample, the A647 photobleached at a rate of 0.04 min^{-1}. The A555 PL intensity increased by ~100% in parallel, and the QD520 PL intensity was constant within approximately ±10%.

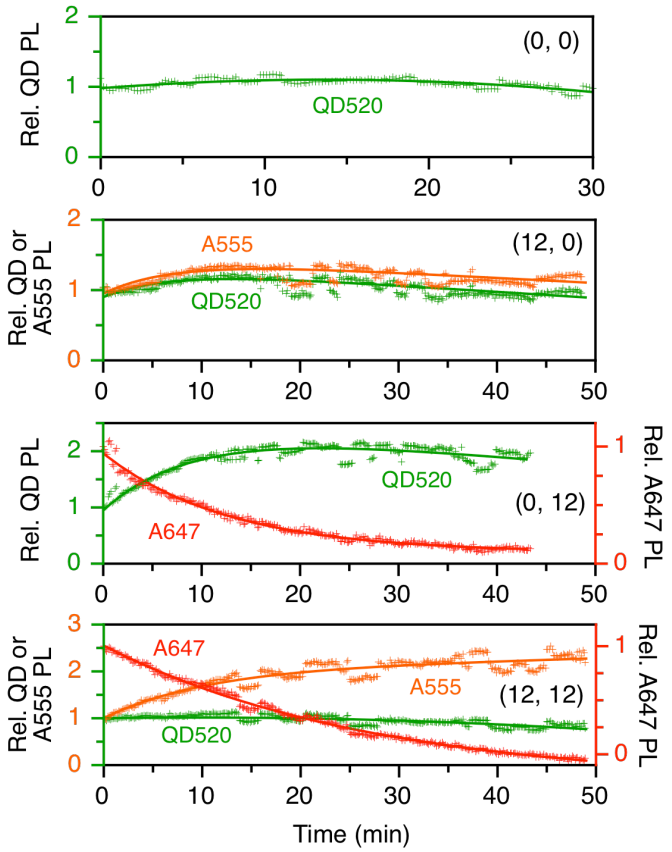

Figure S5. (A) Relative stabilities of the QD520, A555, and A647 PL (as applicable) in the (0, 0), (12, 0), (0, 12), and (12, 12) permutations of the QD520-[Pep(A555)]$_M$-[Pep(A647)]$_N$ cFRET configuration with continuous illumination at 400 nm. The measured power at the sample was ~10 mW, except for the (0, 0) sample, which was ~50 mW. The PL intensities are normalized to an initial value of unity. Note the two different y-axis scales (colour-coded to match the QD520, A555, or A647).

Comparison of Figure S5 with Figure 5 shows that the A647 in the QD520-A555-A647 system photobleached approximately 10-fold more slowly than the A633 and A680 in the QD605-A633-A680 system. However, this direct comparison does not reflect the intrinsic tendency of these dyes to photobleach. As noted in the main text, the excitation rate of the QD605 and, by extension, the A633 and A680, was greater than the excitation rate of the QD520 and A647.

The molar absorption coefficients can be used to estimate the relative excitation rates of the QD605 and QD520 at the same excitation flux. The absorption coefficients for the QD605 and QD520 at their excitation wavelengths for photobleaching experiments were ~2 800 000 M^{-1} cm^{-1} (450 nm) and ~114 000 M^{-1} cm^{-1}(400 nm), respectively. When these values are scaled by

the FRET efficiencies (80–85% with QD605 versus 55–60% for QD520), the A633 and A680 have an approximately 70-fold larger excitation rate than the A647. The observed 10-fold slower photobleaching of the A647 would then suggest that its intrinsic susceptibility to photobleaching is actually 7-fold higher than the intrinsic susceptibility of A633 and A680. However, the PL excitation spectra of QDs often do not superimpose on their absorption spectra. Significant negative deviations tend to be observed at wavelengths ~75 nm or more shorter than the first exciton peak. In the case of FRET from a QD donor to a dye acceptor, the PL excitation spectrum of a QD may be a better reflection of the FRET-sensitized dye excitation rate. In this case, we approximate an *effective* excitation coefficient by assuming that the magnitude of the first exciton peak in the PL excitation spectrum of a QD is equivalent to the molar absorption coefficient at the first exciton peak. When extrapolated to the excitation wavelengths, the values for QD605 and QD520 were 418 000 M^{-1} cm^{-1} and 102 000 M^{-1} cm^{-1}. When corrected for FRET efficiencies, the estimated excitation rate for A633 and A680 is only 6-fold larger than for A647, which would suggest that the intrinsic susceptibility of A647 to photobleaching is just slightly more than half that of the A633 and A680. The reality may be between the two estimates from absorption and PL excitation spectra, such that the practical difference between the resistance of A647, A633, and A680 to photobleaching is minimal.

PL spectra in serum and blood. Figure S6 and Figure S7 show PL spectra for the QD605-[Pep(A633)]$_M$-[Pep(A680)]$_N$, QD520-[Pep(A555)]$_M$-[Pep(A647)]$_N$, and QD525a-[Pep(A555)]$_M$-[Pep(A647)]$_N$ cFRET configurations in various media. Sample permutations include (0, 0), (12, 0), (0, 12), and (12, 12). Media include buffer, 50% v/v and 90% v/v serum (Figure S6), and 50% v/v and 90% v/v whole blood (Figure S7).

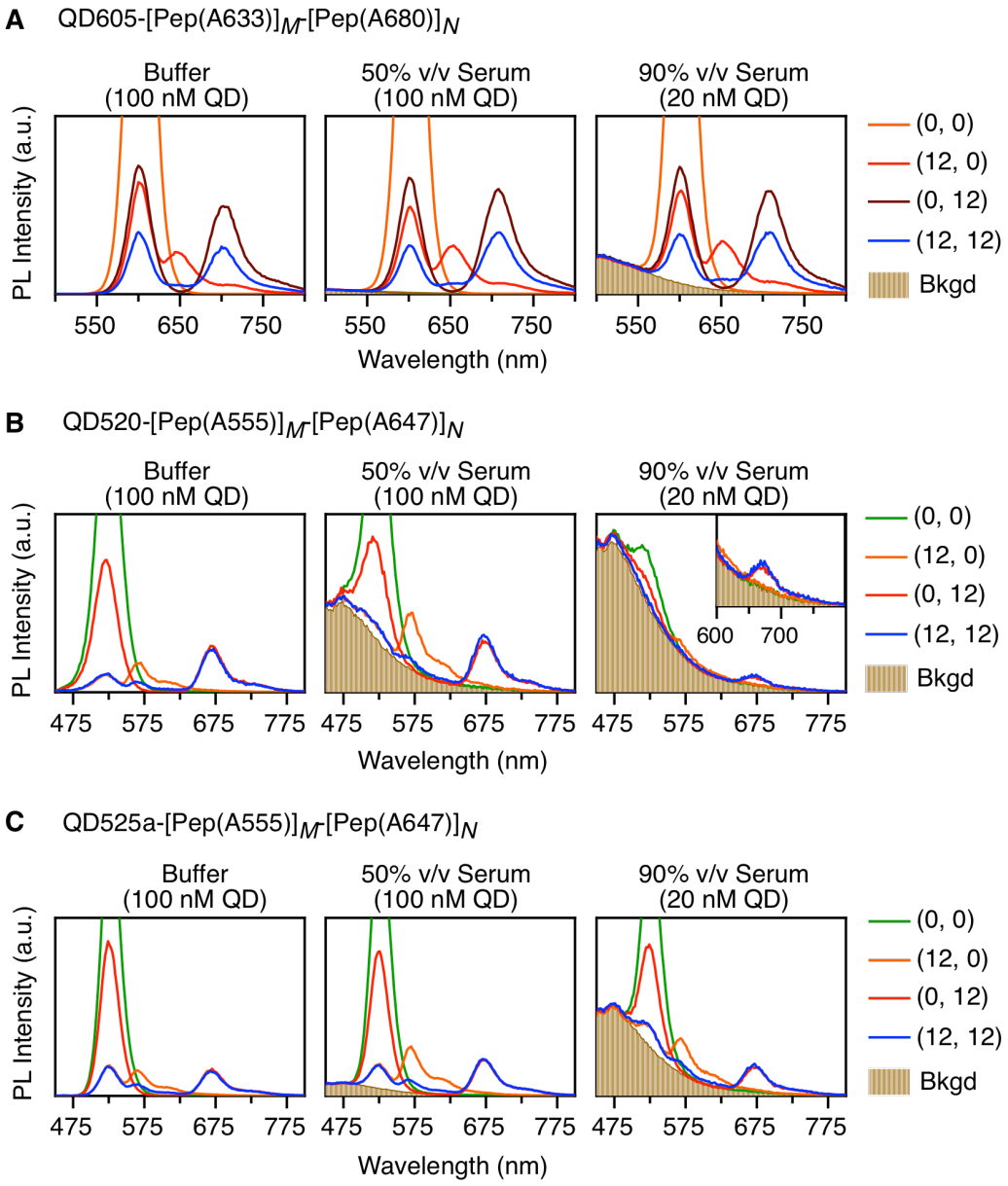

Figure S6. PL spectra for different cFRET configurations and permutations in buffer, 50% v/v serum, and 90% v/v serum. The intensity axis has been set so that the QD PL peaks for the (0, 0) samples are off the scale. These plots are intended to compare the signal-to-background ratios in different media and with different cFRET configurations. The scales of the intensity axes between different plots are not directly comparable.

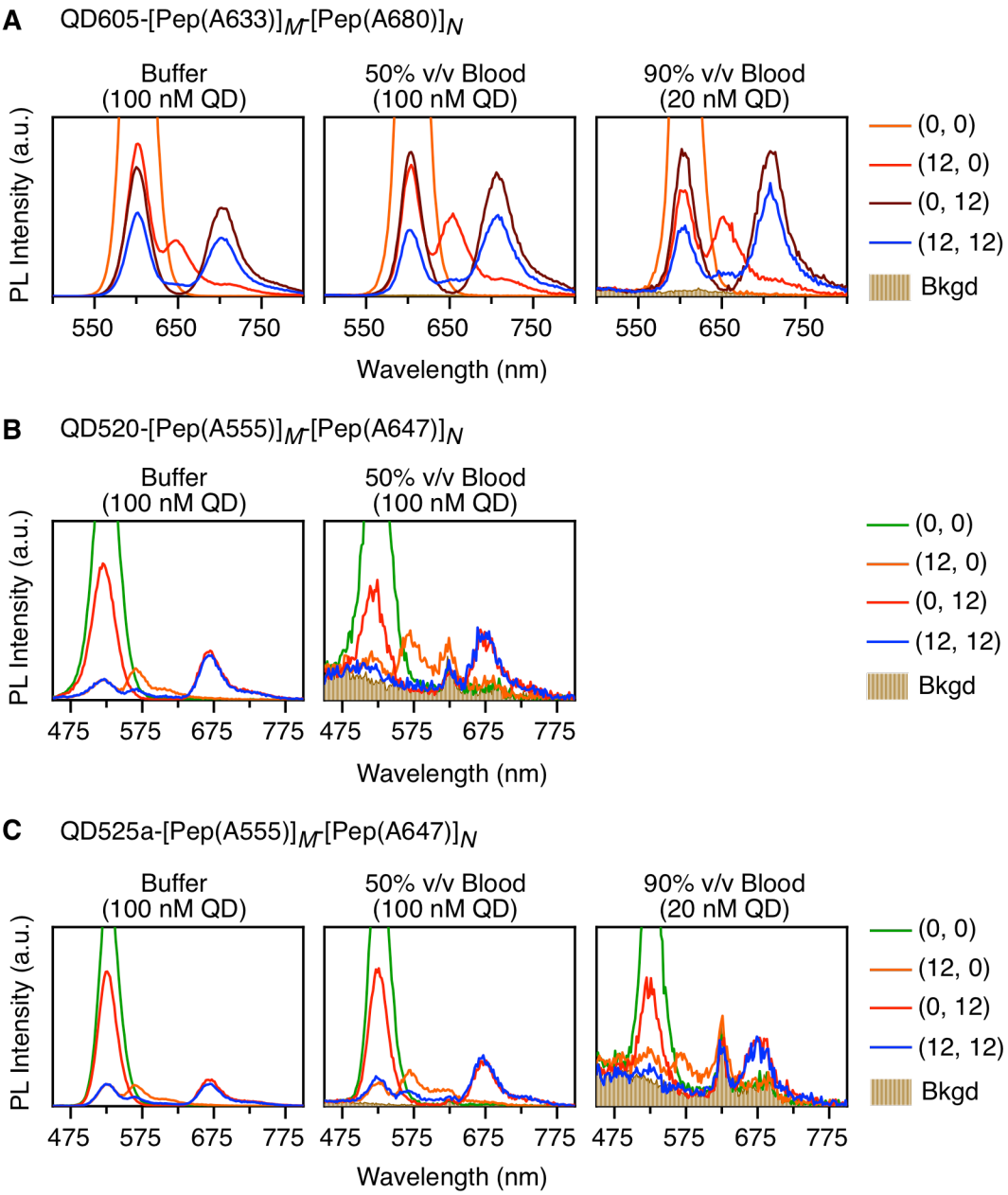

Figure S7. PL spectra for different cFRET configurations and permutations in buffer, 50% v/v blood, and 90% v/v blood. The intensity axis has been set so that the QD PL peaks for the (0, 0) samples are off the scale. These plots are intended to compare the signal-to-background ratios in different media and with different cFRET configurations. The scales of the intensity axes between different plots are not directly comparable. Note: 90% v/v blood was not tested for the QD520 configuration.

Gel electrophoresis of oligonucleotide conjugates. Figure S8 shows agarose gel images that characterize the self-assembly of the dithiol linker-terminated oligonucleotide probes onto the QD605. Figure S8A shows decreases in the electrophoretic mobility of QD605 when mixed with 10 equiv. each of Prb 1 and Prb 2, as well as 15 equiv. each of Prb 1 and Prb 2, in the presence of TCEP. No change in mobility was observed without TCEP. The TCEP-dependent decrease in mobility confirmed that the oligonucleotides assembled on the QDs through the dithiol linker. Without reduction, the disulfide form of the linker had little or no affinity for the QDs. Figure S8B shows the mobility shift for QD605 when mixed with 10 equiv. each of Prb 1 and Prb 2, both before and after salt aging. The retention of a narrow band after salt aging suggests the absence of aggregates, and is another indication that the QD605 were successfully modified with oligonucleotides. Unmodified QDs will often aggregate at such high ionic strength, leading to smearing and/or poor mobility in the gel. There was also a small decrease in the mobility of the band after salt aging, which suggested the assembly of more oligonucleotides per QD. (Note that the decrease in mobility from increased size with assembly of additional oligonucleotides is partially offset by an increase in mobility from increased charge.) The assembly of more oligonucleotides after salt aging was confirmed by hybridizing the oligonucloetide probes with their complements in the presence of SYBR green, a fluorescent stain for dsDNA, as shown in Figure S8C-D. Analysis of the PL images of gels before and after salt aging showed that the relative SYBR green fluorescence from the unassembled oligonucleotide band decreased by ~25% relative to the PL of the QD band. When compared to control lanes with SYBR green-stained double-stranded oligonucleotides without QD605, the relative PL signal for the unassembled oligonucleotide decreased by ~20% after salt aging.

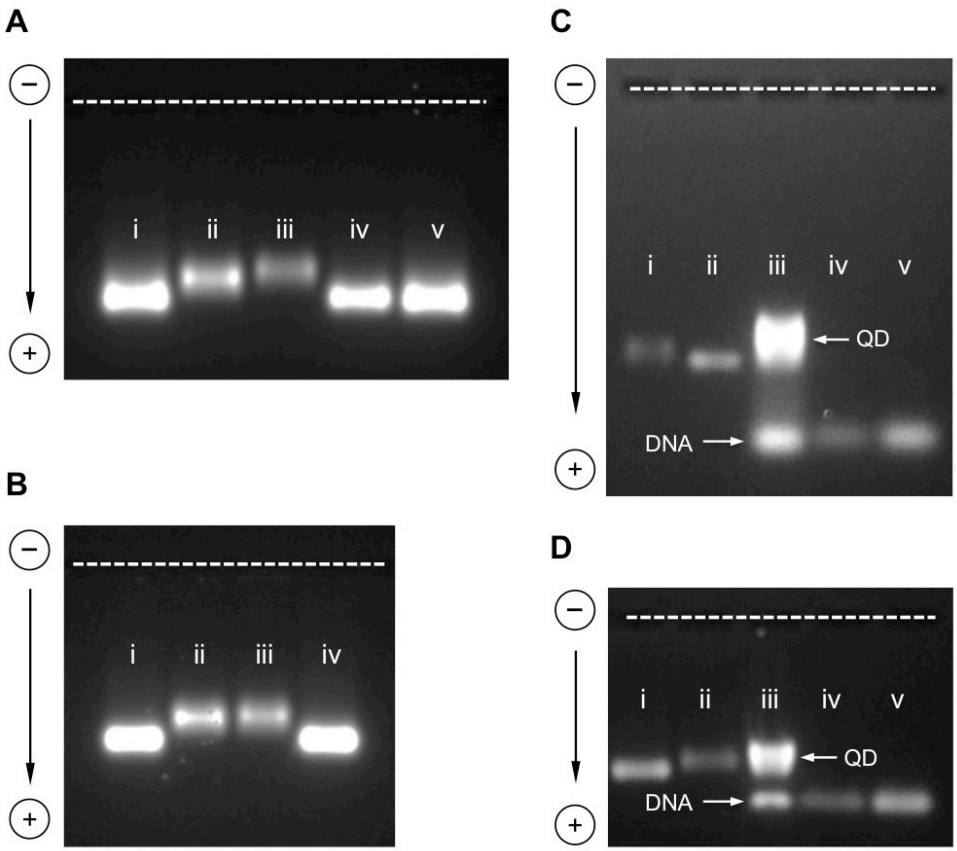

Figure S8. (A) PL image of an agarose gel showing the electrophoretic mobility of QD605-[Prb 1]-[Prb 2] conjugates: (i) $P_1 = P_2 = 0$; (ii) $P_1 = P_2 = 10$ with TCEP; (iii) $P_1 = P_2 = 15$ with TCEP; (iv) $P_1 = P_2 = 15$ without TCEP; (v) $P_1 = P_2 = 0$. Assembly is not 100% efficient (unlike polyhistidine terminated peptides, which approach 100% efficiency); **(B)** PL image of an agarose gel showing the electrophoretic mobilities for (i) $P_1 = P_2 = 0$; (ii) $P_1 = P_2 = 10$ (pre-salt aging); (iii) $P_1 = P_2 = 10$ (post-salt aging); (iv) $P_1 = P_2 = 0$. **(C)** PL images of an agarose gel stained with SYBR green for conjugate samples pre-salt aging: (i) QD605-[Prb 1] conjugates ($P = 10$); (ii) QD; (iii) QD605-[Prb 1] conjugates ($P = 10$) with Tgt 1 and SYBR green; (iv) 20% and (v) 40% Prb 1/Tgt 1 (no QD) with SYBR green. **(D)** PL images of an agarose gel stained with SYBR green for conjugate samples post-salt aging: (i) QD; (ii) QD605-[Prb 1] conjugates ($P = 10$); (iii) QD605-[Prb 1] conjugates ($P = 10$) with Tgt 1 and SYBR green; (iv) 20% and (v) 40% Prb 1/Tgt 1 (no QD) with SYBR green. Images in panels C and D were acquired with a color digital camera under long-wave UV light. The green channel was isolated in Image J for analysis. SYBR green and QD605 both give strong signals in the green channel.

Hybridization and displacement assays. Figure S9 shows changes in FRET efficiency and PL ratios for two batches of QD605-[Prb 1]-[Prb 2] conjugates. One batch was prepared with $P_1 = P_2 = 10$, and the other was prepared with $P_1 = P_2 = 15$, and the probes were hybridized with increasing amounts of either Blk 1(A633) or Blk 2(A680). The FRET efficiencies and PL ratios

for both batches of probe parallel one another until the PL ratios saturate at a lower value for $P_1 = P_2 = 10$. In addition to gel electrophoresis results, these data also show that the number of probes assembled per QD is less than the number mixed, P, and that increasing the value of P increases the final number of probes per QD. For $P = 15$, the number of probes assembled was *ca.* 12, and for $P = 12$, the number of probes assembled was *ca.* 9.

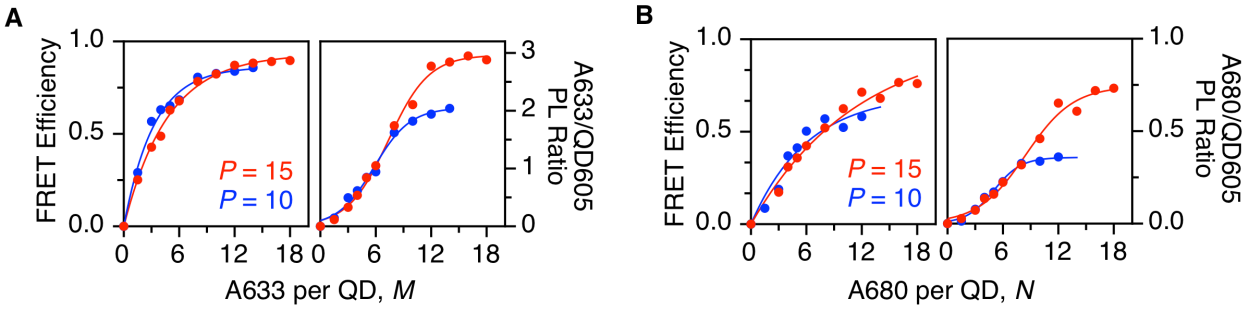

Figure S9. Changes in FRET efficiency and PL ratio with hybridization of QD605-[Prb 1]-[Prb 2] conjugates with **(A)** Blk 1(A633) and **(B)** Blk 2(A680).

Figures S10 and S11 show three-dimensional plots of the A633/QD605 and A680/QD605 PL ratio data plotted in two dimensions in Figures 7A(iii) and 7B(ii).

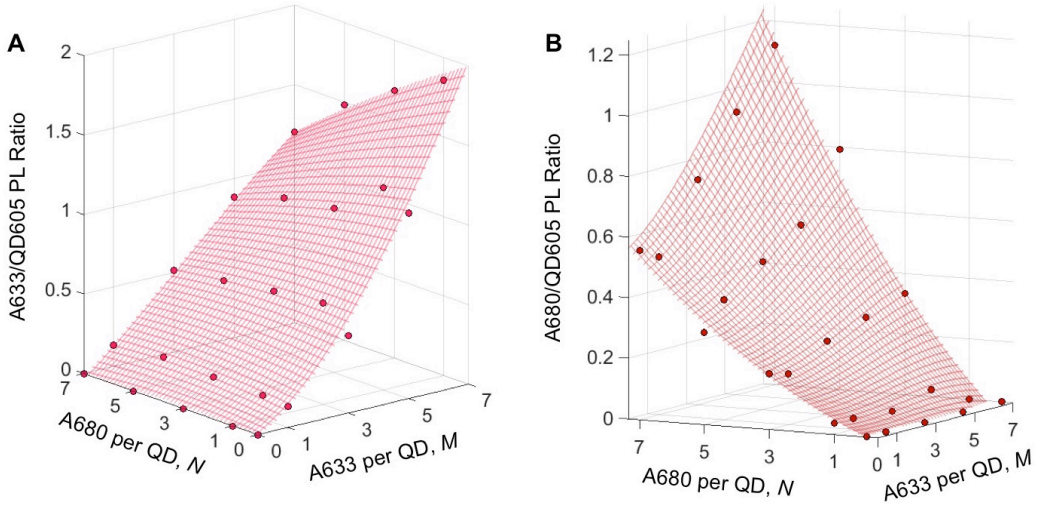

Figure S10. Three-dimensional plots of the calibration data in Figure 7A(iii): **(A)** A633/QD605 PL ratio and **(B)** A680/QD605 PL ratio.

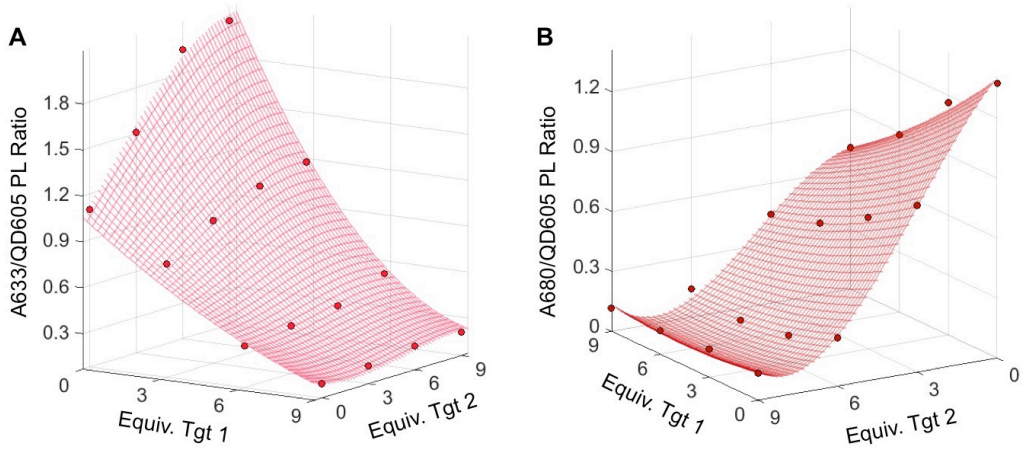

Figure S11. Three-dimensional plots of the calibration data in Figure 7B(ii): **(A)** A633/QD605 PL ratio and **(B)** A680/QD605 PL ratio. The data was fit with polynomial surfaces to permit calculation of the number of equivalents of target in unknown samples from the measured PL ratios.

Additional References

1. W. R. Algar and U. J. Krull, *Sensors*, 2011, 11, 6214-6236.
2. J. Q. Umberger and V. K. Lamer, *J. Am. Chem. Soc.*, 1945, 67, 1099-1109.
3. Sulfo-Cyanine 5 NHS ester, Lumiprobe Inc., http://www.lumiprobe.com/p/sulfo-cy5-nhs-ester, acessed February 27, 2016.